Microbiology and Immunology

Microbiology and Immunology

ORIGINAL ARTICLE OPEN ACCESS

Generation of Replication-Competent Hepatitis B Virus Harboring Tagged Polymerase for Visualization and Quantification of the Infection

Chiharu Morita[1] | Masami Wada[1] | Eriko Ohsaki[1,2] | Shihoko Kimura-Ohba[1] | Keiji Ueda[1]

[1]Division of Virology, Department of Microbiology and Immunology, Osaka University Graduate School of Medicine, Osaka, Japan | [2]Center for Infectious Disease Education and Research (CiDER), Osaka, Japan

Correspondence: Keiji Ueda (kueda@virus.med.osaka-u.ac.jp)

Received: 20 October 2024 | **Revised:** 3 November 2024 | **Accepted:** 4 November 2024

Funding: This research was supported by Grants from the Japan Agency for Medical Research and Development (AMED) Grants (16fk0310504h0005, 17fk0310105h0001, 18fk0310105h0002, 19fk0310105h0003, 20fk0310105h0004, 21fk0310105h005, 22fk0310505h0001, 23fk0310505h0002, and 24fk0310505h003) to K.U. and from JST SPRING, Grant Number JPMJSP2138, to C.M. and from the Osaka University Transdisciplinary Program for Biomedical Entrepreneurship and Innovation (WISE program) to C.M.

Keywords: HBV polymerase | hepatitis B virus | recombinant virus | replication and infection competent | tagged HBV polymerase

ABSTRACT

Hepatitis B virus (HBV) infection is a serious global health problem causing acute and chronic hepatitis and related diseases. Approximately, 296 million patients have been chronically infected with the virus, leading to cirrhosis and hepatocellular carcinoma. Although HBV polymerase (HBVpol, pol) plays a pivotal role in HBV replication and must be a definite therapeutic target. The problems are that the detailed functions and intracellular dynamics of HBVpol remain unclear. Here, we constructed two kinds of tagged HBVpol, PA-tagged and HiBiT-tagged pol, and the HBV-producing vectors. Each PA tag and HiBiT tag were inserted into N-terminus of spacer region on HBVpol open reading frame. Transfection of the plasmids into HepG2 cells led to production of HBV. These tagged HBVpol were detectable in HBV replicating cells and pol-HiBiT enabled quantitative analysis. Furthermore, these recombinant HBV were infectious to primary human hepatocytes. Thus, we successfully designed infectious and replication-competent recombinant HBV harboring detectable tagged HBVpol. Such infectious recombinant HBV will provide a novel tool to study HBVpol dynamics and develop new therapeutics against HBV.

1 | Introduction

HBV infection is one of the most serious global health problems worldwide, with 296 million people chronically infected and 820,000 deaths in 2019 worldwide [1]. Persistent HBV infection causes not only acute hepatitis but also chronic hepatitis leading to cirrhosis and hepatocellular carcinoma [2–4]. However, current treatments are not effective enough to eradicate HBV completely and still have some concerns such as drug resistance due to mutations and requirement of lifelong administration [2]. Thus, we need to understand more detailed lifecycle of HBV to develop new therapeutics against the virus.

Abbreviations: aa, amino acids; Ab, antibodiy; bp, base pair; BSA, bovine serum albmin; cccDNA, covalentaly closed circular DNA; CsCl, cesium chloride; DAPI, 4′6-diamidino-2-phenylindole; DIG, digoxigenin; dslDNA, double-stranded liner DNA; ELISA, enzyme-linked immunosorbent assay; ETV, entecavir; FBS, fetal bovin serum; Fr., fraction; GEI, genome equivalent of infection; GFP, green fluorescent protein; GTC, genotype C; GTD, genotype D; HBcAg, HBV c antigen; HBeAg, HBV e antigen; HBsAg, HBV s antigen; HBV, Hepatitis B virus; HIV, human immunodeficiency virus; HRP, horseradish peroxidase; IFA, immunefluorescence Assay; LOIs, lines of interest; LS, large S; nt, nucreotide; ORF, open reading frame; PBS, phosphate-buffered saline; PCI, phenol/chloroform/isoamyl alcohol (25:24:1); PEG, polyethylene glycol; pgRNA, pregenomic RNA or pregenome RNA; pol, polymerase; pol-HiBiT, HiBiT tagged-HBVpol; pol-PA, PA tagged-HBVpol; qPCR, quantitative real-time PCR (qPCR); rcDNA, relaxed circular DNA; recHBV, recombinant HBV; ROIs, regions of interest; RT, reverse transcriptase; SD, standard deviation; SDS, sodium dodecyl sulfate; SDS-PAGE, sodium dodecyl sulfate polyacrylamide gel electrophoresis; SS, small S; ssDNA, single-stranded DNA; TBS, tris-bufferd saline; TP, terminal protein; WB, western blotting; WT, wildtype.

HBVpol must be a potential therapeutic target because it is the only product with enzymatic activity among HBV proteins and plays a key role in HBV replication. After HBV enters hepatocytes, the HBV genome, partially double-stranded relaxed circular DNA (rcDNA) is converted into covalently closed circular DNA (cccDNA) on the process to nuclear transport. The cccDNA is transcription-competent and viral mRNAs including pregenomic RNA (pgRNA) is produced [5]. pgRNA is not only translated into core and pol but also used as an RNA template that is reversely transcribed into minus strand of HBV DNA and finally into rcDNA by HBVpol [5, 6].

HBVpol consists of four domains, that is, terminal protein (TP), spacer, reverse transcriptase (RT), and RNaseH (Figure 1a) [7–9]. TP domain is essential for initiation of minus strand HBV DNA synthesis through interaction between a packaging signal, ε of pgRNA and HBVpol [10–12]. Spacer domain flacked by TP and RT domain seems dispensable for the activity of reverse transcriptase [8, 13], and probably just functions tethers TP and RT. Actually, sequences of the spacer domain are less conserved in the variant, and there is possibility to put a tag into the region [14]. On the other hand, it overlaps with the preS1 region, which exerts selective pressure on S ORF [8, 15–17]. RT domain has catalytic function as a reverse transcriptase [8, 10, 18, 19]. RNaseH domain works for RNA degradation in the process of reverse transcription [20, 21]. Thus, though most of domains in HBVpol except spacer domain play an essential role during HBV replication, spacer domain could be somewhat tolerant of mutation [8, 16, 17]. Since HBVpol must be a potential HBV therapeutic target [22], we need to know more about the HBVpol. Probably, due to low expression of HBVpol during the viral replication, the detailed functions and intracellular dynamics of HBVpol in the viral life cycle and host interacting factors remain poorly understood [23].

HBV genome is a compact circularized DNA, 3.2 kb long in which four genes are encoded and the ORFs are overlapped each other. Thus, it is very difficult to manipulate the genome to insert some traceable tag like fluorescent proteins such as green fluorescent protein (GFP) and construct a traceable infectious recombinant HBV. There is some possibility to insert a short tag such as HA (9 amino acid [aa]), V5 (14 aa), and so on into the non-overlap regions but the detection efficiency and specificity could be very poor and so far, few reports have been published [24–26]. Moreover, although several tags were inserted into N-terminus or C-terminus of HBVpol in some reports [27, 28], production of recombinant HBV harboring these tagged HBVpol would be quite tough due to overlapping with other genes in the N-terminus and C-terminus of HBVpol.

In this study, we succeeded to establish an infectious recombinant HBV harboring PA- or HiBiT- tagged HBVpol, pol-PA, and pol-HiBiT, respectively, which enabled HBV infection easily tractable and quantitative.

2 | Materials and Methods

2.1 | Cells

HepG2-NTCP (NTCP/G2) cells [29] were maintained in William's medium E medium supplemented with 10% fetal bovine serum (FBS) (Sigma-Aldrich), 50 μM hydrocortisone (Sigma-Aldrich), 5 μg/mL transferrin (Wako Pure Chemicals), 10 ng/mL human epidermal growth factor (Thermo Fisher), 5 μg/mL human insulin (Sigma-Aldrich), 5 ng/mL sodium selenite (Sigma-Aldrich), 2 mM L-glutamine (Nacalai Tesque), 0.5 mg/ml G418, and 1% antibiotic-antimycotic solution (100 units/mL penicillin, 100 μg/mL streptomycin, 0.25 μg/mL amphotericin B) (Nakalai Tesque).

HEK293T cells (Takara-Clontech) were maintained in Dulbecco's Modified Eagle Medium (DMEM) (High Glucose) with 10% FBS (Sigma-Aldrich) and 1% antibiotic-antimycotic solution as above.

Human primary hepatocytes (PXB cells) were purchased from PhoenixBio Co. Ltd. and maintained in the optimized medium which were prepared according to the composition provided by the manufacturer [30].

2.2 | Plasmids

For construction of HBVpol expressing plasmids, HBVpol sequences were amplified from HBV-adr4-producing vector, pHB WT [31, 32] using primers, LVSIN EF1α pol-Fw, and LVSIN pol-Rv and then subcloned into pLVSIN EF1α vector (Takara) treated with XbaI and BamHI restriction enzyme by homologous recombination using In-Fusion HD Cloning Kit (Takara). Based on HBV adr4 sequence, a PA-tag (5′-ggcgttgccatgccaggtgccgaagatgatgtggtg-3′, 36 base pair [bp]; GVAMPGAEDDVV, 12 aa) and a HiBiT-tag (5′-gtgagcggctggcggctgttcaagaagattagc-3′, 33 bp; VSGWRLFKKIS, 11 aa) inserted HBV pol from BstEII to XhoI sites were purchased from GeneArt Custom Gene Synthesis (Invitorogen) as pMARQ pol-PA and pMARQ pol-HiBiT, and the fragments of pol-PA and pol-HiBiT from BstEII to XhoI were replaced with the same site of an HBV-producing vector (pHBV pol-WT) gifted by Dr. Ono from RIMD/CiDER (#AB246345.1) [33, 34] and as resulted, HBV-producing vectors, pHBV pol-PA and pHBV pol-HiBiT were constructed. pol-PA and pol-HiBiT were amplified using primers (LVSIN EF1α pol-Fw, LVSIN pol-Rv) using pHBV pol-PA and pHBV pol-HiBiT as templates, respectively. Then each fragment was subcloned into a pLVSIN EF1α vector treated with XbaI and BamHI with In-Fusion HD Cloning Kit as above and pLVSIN pol-PA and pLVSIN pol-HiBiT were established.

PA-GFP sequences and HiBiT-GFP sequences were amplified using pcDNA3 HA-GFP, which was gifted from Dr. Honda (Okayama university), as a template, using each set of primers (PAGFP-Fw and PAGFP-Rv, HiBiTGFP-Fw and pLVSIN GFP-Rv). The amplified fragment was subcloned into pLVSIN EF1α vector treated with XbaI and BamHI with ligation high v2 (TOYOBO) or In-Fusion HD Cloning Kit, respectively, and pLVSIN EF1α PA-GFP and pLVSIN EF1α HiBiT-GFP were constructed.

To prepare an HBVpol-innactivated HBV-producing vector (pHBV pol dead), a point mutation (Threonine to stop codon at 163 aa in the POL ORF) was introduced into pol of pHBV pol-WT by mutagenesis. Briefly, pHBV pol-WT sequences were amplified using a set of primers (pol dead -Fw, pGEM pol dead-Rv) and then liner pHBV WT fragment harboring mutation on POL ORF

was synthesized. This PCR product was treated with DpnI to remove template plasmids, and then treated with T4 Polynucleotide Kinase (Takara) to add a γ-phosphate group of ATPs to the 5′ end of this fragment for the self-ligation.

For construction of a large S (LS) expressing plasmid (pLVSIN LS), LS sequence was amplified using primers (LVSIN-LHBs-Fw, LVSIN-LHBs-Rv) with pHB WT as a template, then subcloned into a pLVSIN EF1α vector

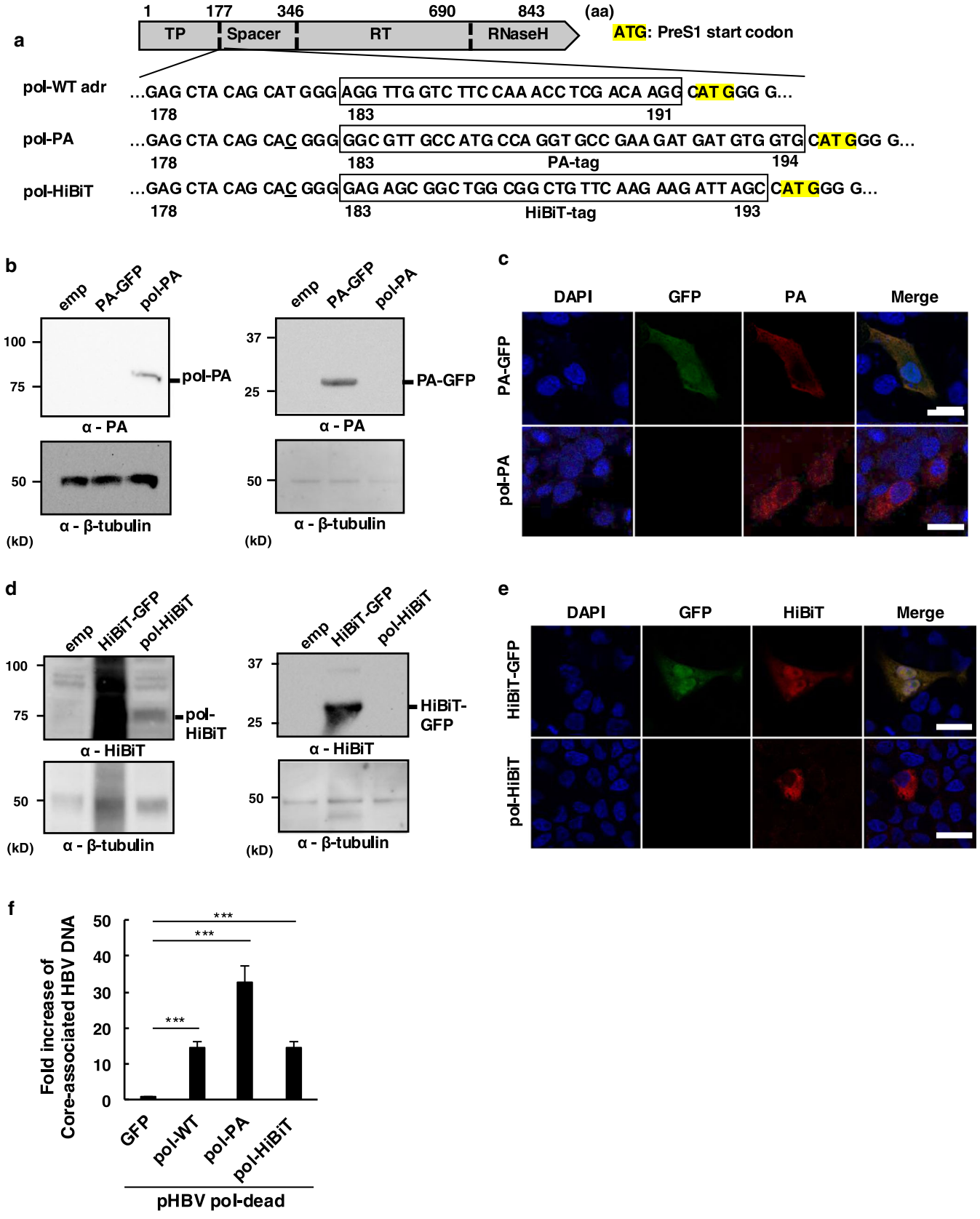

FIGURE 1 | Legend on next page.

treated with XbaI and BamHI using In-Fusion HD Cloning Kit.

Nanoluc sequence was amplified using a set of primers (Hind3-NanoLuc-Fw, NanoLuc-Rv-BamH1) with pNL1.3 (Promega) as a template and then subcloned into a pcDNA3 vector (Invitrogen) treated with HindIII and BamHI by ligation, and pcDNA3 NL1.3 was established. pRL-TK harboring renilla luciferase gene was purchased from Promega.

2.3 | Western Blot Analysis

One day after seeding of HEK293T cells on 12-well plate at 5×10^5 cells/well, cells were transfected with each plasmids using Lipofectamine 2000 (Invitrogen) according to the manufacturer's protocol. NTCP/G2 cells were seeded on 12-well plate at 5×10^5 cells/well and cells were transfected with each pHBV vector using GENJet for HepG2 DNA in vitro Transfection Reagent (SignaGen) according to the manufacturer's protocol.

Two days after transfection, the cells were lysed in a 1 × Sodium Dodecyl Sulfate (SDS) sample buffer (0.125 M Tris-HCl pH 6.8, 4% SDS, 20% Glycerol, 0.01% bromophenol blue and 5% 2-Mercaptoethanol). The lysed samples were boiled at 98°C for 5 minutes (min) and separated by sodium dodecyl sulfate polyacrylamide gel electrophoresis (SDS-PAGE) and transferred to a polyvinyl difluoride membrane (Bio-Rad Laboratories). The membrane was then blocked with 5% skim milk (Nacalai Tesque) in Tris-buffered saline containing 0.1% NP40 (20 mM Tris-HCl, pH 7.6, 150 mM NaCl, 0.1% Tween 20) (TBS-T) for 30 min and probed overnight at 4°C with appropriate antibodies. The next day, the membrane was washed three times with TBS-T for 5 min each and further incubated with either secondary anti-mouse IgG or anti-rabbit IgG conjugated with horseradish peroxidase (HRP) (Dako) for 2 h at 4°C. Then, the chemiluminescence was generated with SuperSignal West Atto Ultimate Sensitivity Substrate (Thermo Fisher Scientific) and detected with ChemiDoc Touch MP (Bio-Rad Laboratories).

In some cases, after first probing, antibodies on the membrane were stripped with WB Stripping Solution or WB Stripping Solution Strong (Nacalai Tesque), then the membrane was re-probed with the other primary antibodies followed by second antibodies and the chemiluminescence signal was detected in the same way.

2.4 | Immunofluorescence Assay (IFA)

For pol-PA or pol-HiBiT detection, 48 h post-transfection of either pol-PA or pol-HiBiT expressing plasmid into NTCP/G2 cells, the cells were fixed with 4% paraformaldehyde in phosphate-buffered saline without Ca and Mg (PBS; 137 mM NaCl, 2.7 mM KCl, 10 mM Na_2KHPO_4, 1.8 mM KH_2PO_4, pH 7.4), and permeabilized with 0.1% Triton X-100 in PBS for 20 min at room temperature, followed by washing with PBS three times. After blocking with 1% BSA (bovine serum albumin) in PBS, the cells were then probed with either an anti-PA monoclonal antibody or an anti-HiBiT antibody, diluted in PBS-0.1% Tween 20 (PBS-T) containing 1% BSA. After washing with PBS-T three times for 5 min each, the cells were incubated with secondary antibodies conjugated with Alexa Fluor 546. Finally, washing as above, the cells were mounted with a 4'6-diamidino-2-phenylindole (DAPI)-containing glycerol solution (Fluoro-KEPPER Antifade Reagent; Nacalai Tesque). The images were obtained with a laser scanning confocal microscope (Leica TCS SP8).

In case of pHBV-transfected cells, cells were seeded on a glass bottom 60 mm dish (MatTek) at 1×10^6 cells/dish. 48 h post-transfection of pHBV pol-PA into NTCP/G2 cells, the cells were fixed, permeabilized, and blocked in the same way as above. The cells were incubated with both an anti-PA antibody and an anti-HBc antibody, followed by incubation with secondary antibodies conjugated with Alexa Fluor 488 or 546. After probing with antibodies and washing, the cells were stained with DAPI (Thermo Fisher Scientific, 1 μg/mL at final concentration) in PBS-T, and then washing the cells with PBS three times for 5 min each and soaked in PBS without mounting. The image was obtained with a laser scanning confocal microscope (Leica: STELLARIS 8).

FIGURE 1 | Expression and detection of PA- or HiBiT- tagged HBVpol. (a) Schematic representation of the expression construction of the tagged HBVpol. Amino acids from 183 to 191 aa of HBV wildtype (WT)-HBVpol (genotype adr) were replaced into a PA-tag (PA) or a HiBiTtag (HiBiT). Here, each start codon of preS1 is highlighted. (b) Western blot of PA-tagged GFP and HBVpol with an anti-PA antibody. 48 h after transfection of either an empty vector (emp), a PA-tagged GFP expressing plasmid (PA-GFP) or a pol-PA expressing plasmid (pol-PA) into HEK293T cell, the cell lysates were prepared for SDS-PAGE followed by Western blot. Electrophoresis was on 7% (left) or 12% (right) gel, respectively. Loading samples were diluted for detection of PA-GFP. As the internal control, β-tubulin was detected using an anti-β-tubulin antibody. (c) Immunofluorescence assay of PA-GFP and pol-PA. 48 h after transfection of either a PA-GFP or a pol-PA expressing plasmid into NTCP/G2 cells, the cell was fixed, permeabilized, and stained with a rat monoclonal anti-PA antibody followed by anti-rat antibodies conjugated with Alexa Fluor 546 (red). (d) Detection of HiBiT-tagged GFP and pol-HiBiT using an anti-HiBiT antibody with Western blot. 48 h after transfection of either an empty vector (emp), a HiBiT tagged-GFP expressing plasmid (HiBiT-GFP) or a pol-HiBiT expressing plasmid (pol-HiBiT) into HEK293T cell, the cell lysates were loaded by electrophoresis in the same way. Loading samples were diluted for the detection of HiBiT-GFP. (d) Immunofluorescence assay of HiBiT-GFP and pol-HiBiT expressing NTCP/G2 cells. The cells were treated as above and stained with a mouse monoclonal anti-HiBiT antibody followed by anti-mouse antibodies conjugated with Alexa Fluor 546 (red). In the IFA (c and e), GFP signal was also obtained. The nucleus was counter-stained with DAPI (blue). Original magnification was 63 × objectives. Scale bar shows 20 nm (white). (f) Trans-complementation analysis for verification of catalytic activity of pol-PA and pol-HiBiT. An HBVpol inactivated HBV-producing vector (pHBV pol-dead) and HBVpol expressing plasmids (pol-WT, pol-PA, and pol-HiBiT) were co-transfected into NTCP/G2 cells. Core-associated HBV DNA of 6 days post-transfected cells was quantified by qPCR. Data were presented as a mean + SD. Asterisks indicate significant differences between negative control (GFP) and each HBVpol expressing cells (Steel test; $N = 3$; $^{***}p < 0.001$).

2.5 | Analysis of IFA Images

The images taken by a laser scanning confocal microscope were analyzed with a Leica Application Suite X software (LasX, Leica). To suppress the blurred images and acquire the high-resolution images, deconvolution processing was performed using a Lightning software (Leica) on STELLARIS 8, and then the brightness was adjusted evenly. Lines of interest (LOIs) were selected randomly and the fluorescence intensity of each using raw image data was measured by a LasX software.

To evaluate the colocalization between green and red fluorescence, the brightness and contrast were adjusted evenly by LasX and subsequently analyzed by Coloc2 plugins on ImageJ Fiji. Regions of interest (ROIs) were selected randomly, and Manders' colocalization coefficient [35, 36] of each LOIs was determined using an automatic threshold.

2.6 | CsCl Density Profile of HBV Particles

NTCP/G2 cells were transfected with 10 μg of each pHBV vector or 7.5 μg of pHBV pol-PA and 2.5 μg of LS protein-expressing plasmid using 30 μL of GENJet for HepG2 DNA in vitro Transfection Reagent (SignaGen) a day after seeding on 10 cm dish at 5.5×10^6 cells/dish. Six days post-transfection, HBV particles in the supernatants of NTCP/G2 cells transfected with respective pHBV WT, pHBV pol-PA, both pHBV pol-PA and LS expressing plasmid and pHBV HiBiT were collected and precipitated with polyethylene glycol (PEG) 8000 (Sigma-Aldrich, 6% at final concentration) overnight at 4°C. After PEG precipitation, the palettes were dissolved well with 500 μL of TBS and centrifuged to remove debris. The cleared concentrated solutions were reacted with 12.5 IU of DNase I (Takara) and 14 μg RNase (Roche Diagnostics) and incubated at 37°C overnight. After this treatment, EDTA (10 mM at the final concentration) was added to inactivate DNase I and the mixture were layered on a CsCl gradient solution (39 F: 350 μL, 35 F: 250 μL, 31 F: 250 μL, 27 F: 250 μL, 23 F: 250 μL and 19 F: 250 μL from the bottom, where F means w/w %). Then, the samples were centrifuged at 50,000 rpm (100,000 × g) at 15°C for 14–20 h using Optima TLX Ultracentrifuge (Beckman coulter). After ultracentrifugation, the samples were fractionated from the top into 14 fractions by 150 μL each. The refraction of each fraction was measured with a refractometer, and the density was calculated according to the equation: g/mL at $25°C = 10.8601 \times \eta - 13.4974$, here η means refraction). Next, HBV s antigen (HBsAg), LS protein (preS1), HBV e antigen (HBeAg), and HBV DNA were measured by ELISA or quantitative PCR.

2.7 | Purification of HBV DNA

To obtain core-associated HBV DNA after transfection, cells were lysed in 1 mL of a hypotonic buffer (20 mM Tris-HCl, pH 7.8, 50 mM NaCl, 5 mM $MgCl_2$, 5 mM $CaCl_2$, 0.1% NP-40, 0.1% β-mercaptoethanol). After freeze and thaw of the lysate, the cleared lysate was obtained by excluding the cell debris. Then 10 U DNase I and 14 μg RNase were added to degrade DNA and RNA outside of the particles. After this treatment, EDTA (10 mM at the final concentration) was added to inactivate DNaseI. Then the mixture was treated with 0.2 mg/mL proteinase K (proK, Roche Diagnostics) after adding SDS at 1.0% and incubated at 56°C overnight. The samples were then subjected to viral DNA extraction using Maxwell RSC Viral Total Nucleic Acid Purification Kit (Promega) and Maxwell RSC Instrument (Promega) according to the manufacturer's instruction. For the preparation of HBV DNA from CsCl fractions, 50 μL of the fraction was treated with proK and then viral DNA was extracted as above.

2.8 | Quantitative Real-Time PCR (qPCR)

To quantify HBV DNA, 2 μL of the extracted core-associated HBV DNA (Σ50 μl) was subjected to real-time PCR using Fast SYBR Green Master Mix (Thermo Fisher Scientific) with a primer set at the S region (HBs-Fw; 5′-cttcatcctgctgctatgcct -3′ and HBs-Rv; 5′-aaagcccaggatgatgggat-3′). The qPCR was monitored with QuantStudio 6 Flex (Thermo Fisher Scientific) and the copy number was elucidated from the standards derived from pHB WT plasmid [31, 32]. The PCR protocol consisted of an initial cycle at 95°C for 20 s, followed by 40 cycles of 95°C for 1 s and 60°C for 20 s, and finally 1 cycle of 95°C for 15 s, 60°C for 1 min, 95°C for 30 s, and 60°C for 15 s.

2.9 | Enzyme-Linked Immunosorbent Assay (ELISA)

HBsAg, LS protein (preS1) and HBeAg in culture supernatants or cell lysates were measured by using commercial ELISA kits (HBs Antigen Quantitative ELISA Kit Rapid-II [Beacle] for HBsAg, HBs Pre-S1 Antigen Quantitative ELISA Kit Rapid [Beacle] and the e Antigen ELISA Kit [Bioneovan] for HBeAg). The HBs ELISA kit detects all kinds of HBs related antigen; large S (LS), middle S (MS), and small S (SS). These were HRP and 3,3′,5,5′-Tetramethylbenzidine based ELISA. Thus, data were colorimetrically obtained by measuring optical density at 450 nm and at 630 nm as a reference and the HBs and LS protein amount were elucidated based on the standard included in the kits.

2.10 | Luciferase Assay

pRL-TK or pcDNA3 Nanoluc was transfected to NTCP/G2 cells for normalization of transfection. Luciferase activities were measured using Renilla-Glo Luciferase Assay System (Promega) and Nano-Glo Luciferase Assay System (Promega), respectively, according to manufacturer's protocol. To measure HiBiT activity, Nano-Glo HiBiT Lytic Detection System (Promega) was used according to manufacturer's protocol.

2.11 | Southern Blotting

The extracted HBV DNA was separated on 1% agarose - Tris-acetate EDTA gel by electrophoresis. Loading amount of each sample was normalized by nanoluc luciferase activity. The separated DNA was

then transferred onto a positively charged nylon membrane (Amersham Hybond-N$^+$ [Cytiva]) using blotting device for hybridization Pad type blotter (TAIMEC). After blotting, the DNA on the membrane was cross-linked with Stratalinker UV 1800 Crosslinker (Stratagene). An HBV-specific probe corresponding to the X region, which was a BamHI and PvuII fragment purified from pHB WT [31, 32], was labeled using DIG DNA Labeling Kit (Roche). Hybridization/washing was performed using a DIG Wash and Block Buffer Set (Roche), according to manufacturer's protocol. Briefly, the DNA blotted membrane was hybridized with DIG labeled DNA probe (11.5 ng/mL at final concentration) at 65°C overnight. After hybridization, the membrane was washed three times for 15 min each and reacted with an anti-Digoxigenin (DIG)-POD, Fab fragments (Roche, 1:10000), and CDP-Star (Roche) was used as chemiluminescent substrate. Images of the chemiluminescence were obtained by ChemiDoc Touch MP (Biorad).

2.12 | Northern Blotting

Total RNA from cells was isolated with TRIzol (Thermo Fisher Scientific) and followed phenol/chloroform extraction according to the manufacturer's instructions. Such RNAs were prepared from NTCP/G2 cells 6 days post-transfection with each HBV-producing vector. Then, the RNA was treated with DNase I to degrade contaminated DNA followed by mRNA purification with PolyATtract mRNA Isolation Systems (BioRad) according to manufacturer's instruction. The concentration was measured and 160 μg of polyA$^+$ RNA was separated on a 1% formaldehyde–1.2% agarose gel in a denatured condition. After blotting on a positively charged nylon membrane (Amersham Hybond-N$^+$ [Cytiva]) followed by UV crosslinking, the membrane was probed with a DIG-labeled RNA probe corresponding to the X region (1374 nucleotide [nt] to 1838 nt) of the HBV adr4 genome (GenBank: # LC090200.1) [32] at 65°C overnight. DIG RNA Labeling Kit (Roche) was used for preparation of X region RNA probe. A part of X region sequence amplified using a set of primers (NB-HBV XmRNA-Fw and NB-HBV XmRNA-Rv) was subcloned into a pSPT18 vector (GenBank: A13388.1) treated with XbaI and EcoRI by ligation and then the pSPT18 HBV X were linearized by digestion with HindIII and BamHI and the DNA fragment was purified with PCI extraction followed by ethanol precipitation. RNA polymerase T7 was used for amplification of antisense HBV X mRNA while labeling with a DIG RNA labeling kit (Roche) according to the manufacturer's instruction. After washing as described in Southern blotting, the bound probes were reacted with an anti-digoxigenin-AP conjugated Fab fragment and the luminescence was generated with CDP-Star (Roche). The images were obtained with a ChemiDoc Touch MP or VersaDoc imaging system (BioRad).

The HA GFP expressing plasmid was co-transfected with HBV-producing vectors as a transfection control. HA GFP mRNA was detected using DIG-labeled RNA probes. To prepare this probe, DIG RNA Labeling Kit (Roche) was used. A part of GFP sequence amplified using a set of primers (NB-GFP mRNA-Fw and NB-GFP mRNA-Rv) was subcloned into a pSPT18 vector (GenBank: A13388.1) treated with XbaI and EcoRI using In-Fusion HD Cloning Kit (Takara), then the pSPT18 GFP were linearized by digestion with HindIII and PvuII and the DNA fragment was purified with PCI extraction followed by ethanol precipitation. RNA polymerase SP6 was used for amplification of antisense GFP RNA while labeling with a DIG RNA labeling kit (Roche) according to the manufacturer's instruction. Except probes for GFP, the process of hybridization and washing was done in the same way for detection of HBV DNA.

2.13 | HBV Infection

Human primary hepatocytes (PXB cells) were purchased from PhoenixBio Co. Ltd. seeded at the density of 4×10^5 cells/well on a 24-well plate. The prepared HBV was infected with PXB cells at 0, 100, 500, and 1000 genome equivalent of infection (GEI) in 250 μL of the PXB-optimized medium containing 4% PEG 8000 [37]. The next day, these infected cells were washed with the medium twice and replaced with fresh medium with or without 500 nM of entecavir (ETV). The culture medium was refreshed every 3 days until 12 days postinfection with or without 500 nM of ETV. On the last day, the supernatant was collected to evaluate the amount of HBeAg and core-associated HBV DNA was extracted from the lysate for the qPCR.

2.14 | Antibodies

The following antibodies (Ab) were used in this study; a rat monoclonal anti-PA Ab (FUJIFILM Wako Chemicals Co. 1:700 for Western Blot [WB]; 1:400 for IFA), a mouse monoclonal anti-HiBiT Ab (Promega, 1:1000 for WB and IFA), a mouse monoclonal anti-HBc Ab (Institute of Immunology Co. Ltd. 1:1000 for WB), a mouse monoclonal anti-HBs Ab mono2 (Beacle, 1:1000 for WB), a mouse monoclonal anti-tubulin Ab (Sigma-Aldrich, 1:2000 for WB), and a rat monoclonal anti-HA-Biotin Ab, High Affinity 3F10 (Roche, 1:1000 for WB), a goat anti-rat Ab conjugated with Alexa Fluor 546 (Thermo Fisher Scientific, 1:1000 for IFA), a goat anti-mouse Ab conjugated with Alexa Fluor 546 conjugated (Thermo Fisher Scientific, 1:1000 for IFA), and a donkey anti-rat Ab conjugated with Alexa Fluor Plus 488 (Thermo Fisher Scientific, 1:1000 for IFA).

2.15 | Primers

The following primers were used in this study. LVSIN EF1α pol-Fw; 5′-ggatttaaattctagatgcccctatcttatcaaca-3′, LVSIN pol-Rv; 5′-cggtagaattggatctcacggtggtctccatgc-3′, PA GFP-Fw; 5′-attctagaaccatgggcgttgccatgccaggtgccgaagatgatgtggtggtgagcaagggcgagga-3′, PA GFP-Rv; 5′-atggatccttacttgtacagctcgtccatg-3′, HiBiT GFP-Fw; 5′-attctagaaccatggtgagcggctggcggctgttcaagaagattagcgggagttctggcgtgagcaagggcgagga-3′, pLVSIN GFP-Rv; 5′-cggtagaattggatcttacttgtacagctcgtcc-3′, pol dead-Fw; 5′-tataagagagaaacttaacgcagtgcctcattc-3′, pGEM pol dead-Rv; 5′-tagaatgcccgccttccacaga-3′, Hind III-NanoLuc-Fw; 5′-gtgaagcttatgaactccttctccacaag-3′, NanoLuc-Rv-BamH1; 5′-cacggatcctaccacatttgtagaggtttt-3′, LVSIN-LHBs-Fw; 5′-ggatttaaattctagaccatgggaggttggtcttcc-3′, LVSIN-LHBs-Rv; 5′-cggtagaattggatctcaaatgtatacccaaagaca-3′, NB-HBV XmRNA-Fw; 5′-gcagtctagagctcgcagccggtctggagc-3′, NB-HBV XmRNA-Rv; 5′-accggaattccagtaggacatgaacatgagatgattagg-3′, NB-GFP mRNA-Fw; 5′-gcaggtcgactctaggtgagcaagggcgaggag-3′ and NB-GFP mRNA-Rv; 5′-agggagaccggaattttacttgtacagctcgtcc-3′.

2.16 | Statistical Analysis

Statistical analysis was performed by JMP Pro17 (SAS Institute). Data were presented as a mean + standard deviation (SD) of at least three independent experiments. Student's *t*-test, Dunnett test, Tukey-Kramer test, and Steel test were used to compare the statistical discrepancies among groups. The values of $p < 0.05$ were considered statistically significant ($^{*}p < 0.05$; $^{**}p < 0.01$; $^{***}p < 0.001$ in the figures).

3 | Results

3.1 | Construction of Functional Tagged HBVpol

Given the importance of physiological significance of HBVpol, we predicted that insertion of a tag into spacer domain of HBVpol would have less impact on the function with being visually traceable and/or quantifiable. To this end, we designed PA (GVAMPGAEDDVV, 12 aa) tagged HBVpol (pol-PA) and HiBiT (VSGWRLFKKIS, 11 aa) tagged HBVpol (pol-HiBiT) into the beginning of spacer domain (Figure 1a) in an HBV-producing construct. PA tag is derived from a PLAG sequence of human podoplanin and an anti-PAtag antibody (NZ-1) recognizes the loop structure within proteins with high affinity [38, 39]. The HiBiT tag is a small unit of nanoluc split into two parts and generates luminescence when it interacts with another large subunit, LgBiT (Promega).

The spacer domain was overlapped with the preS1 region of S ORF [15]. In view of this overlapping, we designed the position of insertion in the spacer region (183–191aa) of HBVpol just front of preS1 start codon, though it might affect not only 2.4 kb mRNA transcription for LS protein but also its translation itself (Figure 1a). In addition, the naturally occurred preS1 N-terminus deletion of HBV variants of genotype C (GTC) have been reported. The deletion changed 119 aa preS1 of GTC to 108 aa genotype D (GTD)-like preS1 [40, 41] without affecting the viral replication and infectivity [42, 43]. We first checked expression of pol-PA and pol-HiBiT with transient transfection into HEK293T cells followed by Western blot analysis using tagged HBVpol expression plasmid (pLVSIN pol-PA and pol-HiBiT, respectively). The expressed each tagged HBVpol was easily detected with respective specific antibody (Figure 1b,d) and also with an anti-HBVpol antibody gifted from Dr. Miyakawa from NIID (Supporting Information S1: Figure S1a,b). In IFA, expression of pol-PA and pol-HiBiT were observed in the cytoplasm of pol-PA- and pol-HiBiT- transfected NTCP/G2 cells [29], respectively (Figure 1c,e). The results suggested that pol-PA and pol-HiBiT should be expressed and detected by a specific anti-tag antibody even though each tag inserted into spacer domain.

To assess whether each tagged HBVpol had enzymatic activity as a reverse transcriptase, we next performed a trans-complementation experiment in which an HBVpol-dead HBV-producing vector (pHBV pol-dead) was co-transfected with either a pol-PA or a pol-HiBiT expression plasmid into NTCP/G2 cells (Figure 1f). As a result, the tagged HBVpol definitely complemented intracellular core-associated HBV DNA synthesis, compared with those without HBVpol expression (Figure 1f), though complementation activity seemed variable depending on the type of HBVpol. This data indicated that both recombinants; pol-PA and pol-HiBiT maintained HBVpol activity.

3.2 | Production of Recombinant HBV-Harboring Pol-PA or Pol-HiBiT

To investigate whether recombinant HBV-harboring pol-PA or pol-HiBiT could be produced, we prepared recombinant HBV-producing vectors, pHBV pol-PA, and pHBV pol-HiBiT, respectively. These vectors were constructed based on a wild-type HBV-producing vector (pHBV pol-WT, subtype adr) in which the vectors were designed to produce pgRNA and all the other genes from about 1.2 times HBV genomes (Figure 2a). Each vector was transfected into NTCP/G2 cells, and two days after transfection, extracellular/intracellular HBeAg, extracellular HBsAg, and core-associated DNA were evaluated by ELISA and qPCR. The results showed that HBV antigens were expressed, and core-associated HBV DNA was also detected comparably with HBV WT (Figure 2b-d, Supporting Information S1: S2a). Western blot of the lysates showed comparable HBV core antigen (HBcAg) expression consistently (Supporting Information S1: Figure S2b). These data suggested that recombinant HBV pol-PA and HBV pol-HiBiT should be produced.

Because tags were inserted into the spacer region located upstream of the preS1 translation start codon, ATG (Figures 1a,2a), we next checked the amount of extracellular LS protein with preS1 ELISA. The production of extracellular LS protein was quite lower in the supernatant of pHBV pol-PA- or pHBV pol-HiBiT- transfected cells compared with that of pHBV WT (Figure 2e). Notably, quite a little or no expression of preS1 (LS) was secreted from pHBV pol-PA-transfected cells. Accordingly, Northern blotting showed less expression of 2.4 kb mRNA in pHBV pol-PA-transfected cells (Figure 2f), suggesting that insertion of the tags into such region should affect 2.4 kb mRNA transcription machinery rather than translation.

We next examined the HBV genome replication in the pHBV-transfected cells by detection of core-associated HBV DNA by Southern blotting analysis. Single-stranded DNA (ssDNA), double-stranded linear DNA (dslDNA), and rcDNA were detected in each pHBV-transfected cell (Figure 2g). Production of replicated DNA seemed to be decreased in case of pHBV pol-PA, probably because mature HBV production was reduced due to lower expression of LS. Nevertheless, the results indicated that the HBV pol-PA and HBV pol-HiBiT should be produced as replication-competent HBV.

3.3 | Visual and Quantitative Evaluation of the Expression of PA- or HiBiT-Tagged HBVpol in HBV Replicating Hepatocyte

Since we confirmed that pHBV pol-PA and pol-HiBiT produced replication-competent recombinant HBV, we next tried to detect pol-PA or pol-HiBiT in HBV replicating cells. We performed IFA of NTCP/G2 cells transfected with pHBV

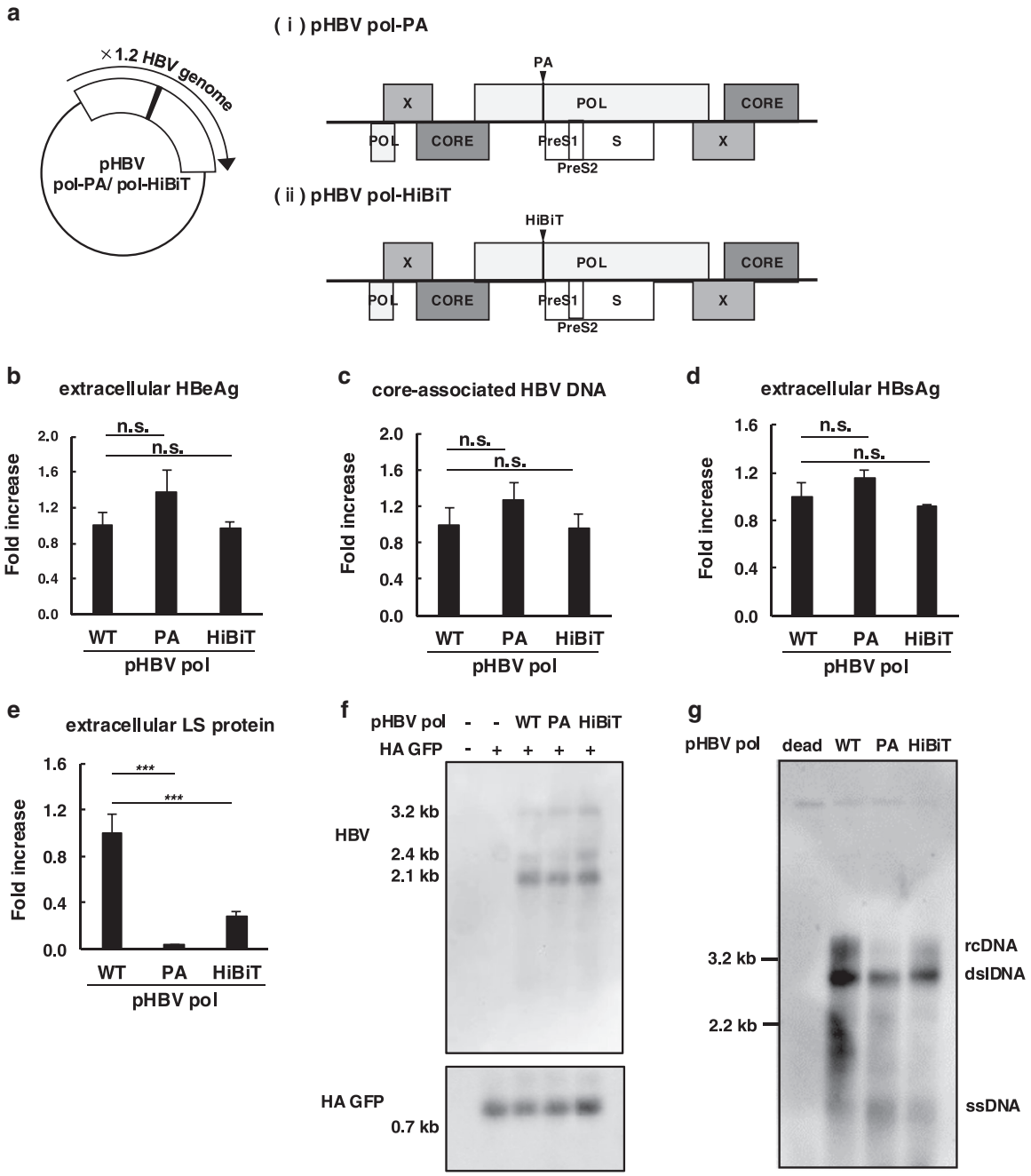

FIGURE 2 | HBV production from pHBV pol-PA or HBV pol-HiBiT producing constructs. (a) Schematic representation of HBV-producing vector with tagged HBVpol; (i) pHBV pol-PA and (ii) pHBV pol-HiBiT. All the ORFs encoded by the HBV genome overlap with the POL ORF. Either a PA tag or a HiBiT tag was inserted and replaced into the designated site of POL ORF in each 1.2-fold HBV-producing vector, and these vectors were hereafter referred to as pHBV pol-PA or pHBV pol-HiBiT, respectively. (b–e) 6 days post-transfection of each pHBV vectors on NTCP/G2 cells, HBeAg in supernatant (b) and the level of core-associated HBV DNA (c) purified from each cell lysates measured by ELISA or qPCR. 48 h post-transfection of each pHBV vectors into NTCP/G2 cells, secreted HBsAg (d) and LS proteins (preS1) (e) were measured by ELISA ($N = 3$). The amount of each antigen and core-associated HBV DNA were normalized by renilla luciferase activity. Non-significant difference was described as "n.s.". (Dunnet test, $N = 3$) Asterisks indicate significant differences between cells (***$p < 0.001$). (f) Northern blot of HBV transcripts in pHBV-transfected NTCP/G2 cells, 48 h after transfection, total RNA was extracted from each pHBV-transfected cell. Poly A^+ RNA was purified from the total RNA by oligo dT conjugated magnetic beads, and then 160 ng of the RNA from each cell was separated on a denatured agarose gel and hybridized with an HBV RNA probe or GFP RNA probe. HA GFP mRNA was detected as a transfection control. (g) Southern blot of replicated HBV DNA in transfected NTCP/G2 cells with each pHBV vector. Core-associated HBV DNA was extracted and purified from the transfected cells. A NanoLuc expressing plasmid was co-transfected with each pHBV vector to normalize the transfection efficiency.

pol-PA or pol-HiBiT. In the HBV life cycle, HBVpol binds with pgRNA and this complex is encapsulated into a capsid [44–46]. Therefore, we hypothesized that HBVpol could be co-localized with capsid. We observed NTCP/G2 cells transfected with pHBV pol-PA by confocal microscopy using an anti-PA antibody and an anti-HBc antibody that preferably detects capsids [47]. As predicted, pol-PA were observed in cytoplasm closed to capsid in HBV replicating NTCP/G2 cells (Figure 3a). The

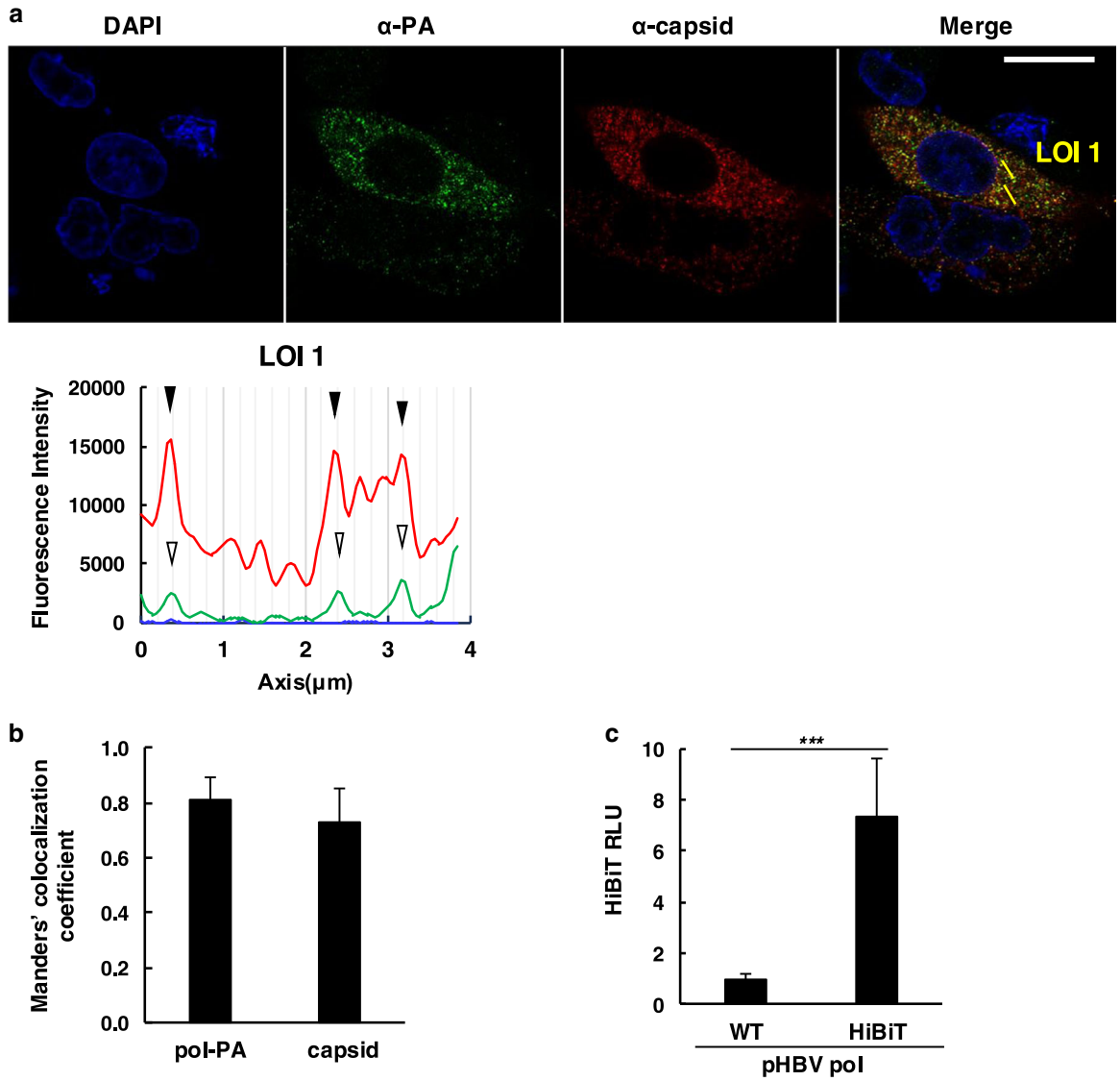

FIGURE 3 | Visual and quantitative detection of pol-PA and pol-HiBiT in HBV replicating cells. (a) Immunofluorescence assay of pol-PA in HBV replicating cell. 48 h after transfection of pHBV pol-PA into NTCP/G2 cells, the cell was prepared for IFA and probed with a rat monoclonal anti-PA antibody and a mouse monoclonal anti-capsid antibody, followed by anti-rat antibodies conjugated with Alexa Fluor 488 (green) and anti-mouse antibodies conjugated with Alexa Fluor 594 (red) respectively. The nucleus was counter-stained with DAPI (blue). Fluorescence intensities of each wavelength were measured using Microscope Imaging Software, Leica Application Suite X (LAS X). The position of the peak with higher red fluorescence was indicated by solid arrowhead, and that with higher green fluorescence was indicated by white arrowhead. Original magnification was 63× objectives. Scale bar shows 20 nm (white). (b) Analysis of colocalization with Manders' correlation coefficients. Four ROIs on three NTCP/G2 cells transfected with pHBV pol-PA ($N = 12$) were determined randomly. Coloc2 application on Fiji-ImageJ automatically calculated M1/M2 and tM1/tM2 values. These values accounts for the total amount of fluorophores that overlap with each other. The more overlap there is, the closer each value is to 1. M1 and M2 indicate the ratio of green/red fluorescence overlapping red/green fluorescence. tM1 and tM2 mean the M1 and M2 values above the Costes threshold. At this time, tM1/tM2 values was showed, and tM1 value (pol-PA) indicated degree to green fluorescence overlapped with red, and tM2 value (capsid) indicated degree to green fluorescence. (c) HiBiT assay of pHBV pol-HiBiT-transfected cell. 48 h after transfection with either pHBV pol-WT or pol-HiBiT into NTCP/G2 cells, HiBiT activity was measured. (student *t*-test, $N = 3$) Asterisks indicate significant differences between cells (***$p < 0.001$).

fluorescence intensity of LOIs was also analyzed with a LasX microscope imaging software. Peak signal of red fluorescence (capsid) overlapped with that of green fluorescence (pol-PA) (Figure 3a, Supporting Information S1: S3a). Furthermore, co-localization between pol-PA and capsid was statistically analyzed by Manders' methods (Figure 3b), which calculates degree of the spatial overlapping between two types of fluorescence [35, 36, 48]. Pol-PA was shown to be highly overlapped with capsid and scored high Manders' value. (Figure 3a,b and Supporting Information S1: S3a). In case of pol-HiBiT, core proteins were detected with rabbit polyclonal antibodies against HBc, because only a mouse monoclonal anti-HiBiT antibody was available, and we could not use a mouse monoclonal anti-HBV capsid antibody. As shown in Supporting Information S1: Figure S3b,c, the IFA fluorescence signals were not completely overlapped but observed rather at

juxtaposition, probably because rabbit polyclonal antibodies against HBc would react with non-assembled core proteins as well as capsids.

As HiBiT tagging system could be easily and quantitatively evaluated by a HiBiT assay, we measured pol-HiBiT in the lysate of NTCP/G2 cells transfected with pHBV pol-HiBiT. Compared with that of pHBV WT-transfected cells, luciferase activity was significantly increased in the pHBV pol-HiBiT-transfected cells (Figure 3c). These results suggested that the construct should be useful for tracking of the HBVpol expression and the quantification in the HBV life cycle.

3.4 | Recombinant HBV Pol-PA and Pol-HiBiT are Produced as Mature Virions

To determine that matured HBV particles were produced from pHBV pol-PA and pol-HiBiT, we performed characterization of HBV particles secreted into cultured medium of pHBV pol-PA and pHBV pol-HiBiT-transfected NTCP/G2 cells. Six days after transfection, HBV particles in the supernatants were collected and concentrated with 6% PEG8000. It was then treated with DNase I and RNase in order to remove plasmids and DNA or RNA outside of HBV particles. The DNase/RNase treated samples were separated 14 fractions with CsCl density gradient ultracentrifugation. The CsCl density of each fraction was calculated from the refractive index, and the amount of HBV DNA with qPCR, and HBsAg, LS protein (preS1) and HBeAg with ELISA in each fraction were measured (Figure 4a,b and Supporting Information S1: S4). The peaks of HBV DNA, HBsAg, and LS protein (preS1) from HBV pol-WT and HBV pol-HiBiT were detected almost in the same fraction (Fr.) with the density around 1.15–1.2 g/mL CsCl (WT: Fr.5-6, HiBiT: Fr.7) (Figure 4a,b). It suggested that mature recombinant HBV (recHBV) particles harboring either pol-WT or pol-HiBiT were produced. Peak of HBV DNA did not overlap with peak of the HBsAg from pHBV pol-PA, and LS protein was not detected (Supporting Information S1: Figure S4). This result was consistent with the result that expression of LS protein was extremely low in pHBV pol-PA-transfected NTCP/G2 cells (Figure 2e, 4e), though global HBsAg expression into supernatant was not affected (Figure 4f). These results suggested that LS expression was considerably impaired in case of pHBV pol-PA. Therefore, we decided to perform LS protein complementation to produce recHBV particles harboring pol-PA. And thus, an LS expressing plasmid (pLVSIN LS) was constructed and co-transfected with pHBV pol-PA. As resulted, intracellular and extracellular LS expression was recovered well as shown in the Western blot and ELISA, respectively. Intracellular SS expression seemed to be reduced in the sole transfection of pHBV pol-PA (Figure 4d), and in contrast, extracellular HBsAg was comparably or more detected with HBsAg-ELISA at 48 h or 6 days post-transfection (Figures 2d, 4f). And intracellular SS protein expression was recovered by co-transfection with pHBV pol-PA and pLVSIN LS, though the reason was unclear (Figure 4d,e).

In the CsCl density gradient ultracentrifugation of LS complemented HBV pol-PA, HBV DNA and HBsAg were detected the most abundantly in the fraction with the density around 1.15–1.2 g/ml CsCl (PA + LS: Fr. 5-6) and LS (preS1) protein as well (Figure 4c). This result showed that LS protein was supplied enough in trans to produce mature recHBV particles from pHBV pol-PA. HBeAg was the highest in the fraction with the density around 1.3 g/mL of the CsCl gradient, which probably reflected capsids leaking out of the transfected cells due to cell damage and so on [49].

To confirm whether such peak fraction really contained replicated HBV DNA or not, HBV DNA in the fraction was extracted and subjected to southern blotting analysis with a specific probe. As shown in Figure 4g, rcDNA was abundantly detected in such fractions with the density of 1.15–1.2 g/mL from HBV pol-WT, HBV pol-PA with additional LS expression, and pol-HiBiT. Taken together, it was found that HBV pol-PA and HBV pol-HiBIT were produced as mature recombinant virions, though HBV pol-PA needed LS supply in trans.

3.5 | HBV Pol-PA and Pol-HiBiT are Infectious to Primary Human Hepatocytes

When some recombinant viruses are designed, it is important to show the infectivity and the ability to produce daughter viruses. We tested whether our designed recHBV was infectious and replication-competent for daughter virion production. In this experiment, primary human hepatocytes (PXB cells), which were prepared from one of humanized mice where the mouse hepatocytes were replaced with human ones [50], were used. The cells were frequently used as an in vitro infection model completely supporting the HBV lifecycle [30, 37, 51]. RecHBV was harvested from the culture medium of NTCP/G2 cells six days after transfection with either pHBV pol-WT, pHBV pol-PA and pLVSIN-LS, or pHBV pol-HiBiT. The viruses were concentrated with 6% PEG8000 and re-dissolved in PBS. After filtration through Amicon Ultra Centrifugal Filter Units 100 K (merck), the solutions were used as infectious HBV stock. Extracellular particle-associated HBV DNA was measured by qPCR to determine the virus titer. PXB cells were incubated with the virus stock at the titer of 0, 100, 500, 1000 GEI. Then, the cells were cultured for twelve days with refreshing the medium every three days. In case 500 nM entecavir was added. This was refreshed also every three days (see Figure 5a,b).

HBeAg in the supernatants was monitored every 3 days till the end. HBeAg secreted from each HBV-infected cells were increased for all the cases in an incubation time-dependent manner. (Figure 5c,e,g). Core-associated HBV DNA in the lysate was increased in a dose-dependent manner and ETV treatment significantly reduced the core-associated HBV DNA, meaning that the DNA was generated according to de novo HBV replication (Figure 5d,f,h). In summary, our recHBV produced from NTCP/G2 cells transfected with either pHBV pol-PA and pLVSIN-LS or pHBV pol-HiBiT were infectious and replication-competent.

4 | Discussion

Current HBV treatments with nucleotide analogs is a life-long treatment and encounters occasionally emergence of drug-resistant viruses leading to re-activation of HBV [52]. Especially, it seems impossible to eradicate cccDNA which is generated

after establishment of HBV infection, though peg-interferon therapy might enhance degradation of cccDNA [2]. These issues and limited therapeutics make it difficult to cure approximately 300 million HBV patients. Thus, development of novel HBV drugs should be facilitated. To address that point, we need more convenient HBV infection systems.

Since the establishment of the reverse genetics for poliovirus and many other viruses have been developed and have contributed to viral research [53, 54]. After the establishment of Human immunodeficiency virus (HIV) molecular clones, HIV research has dramatically developed [55]. In addition, recombinant viruses with inserted reporter genes have contributed to

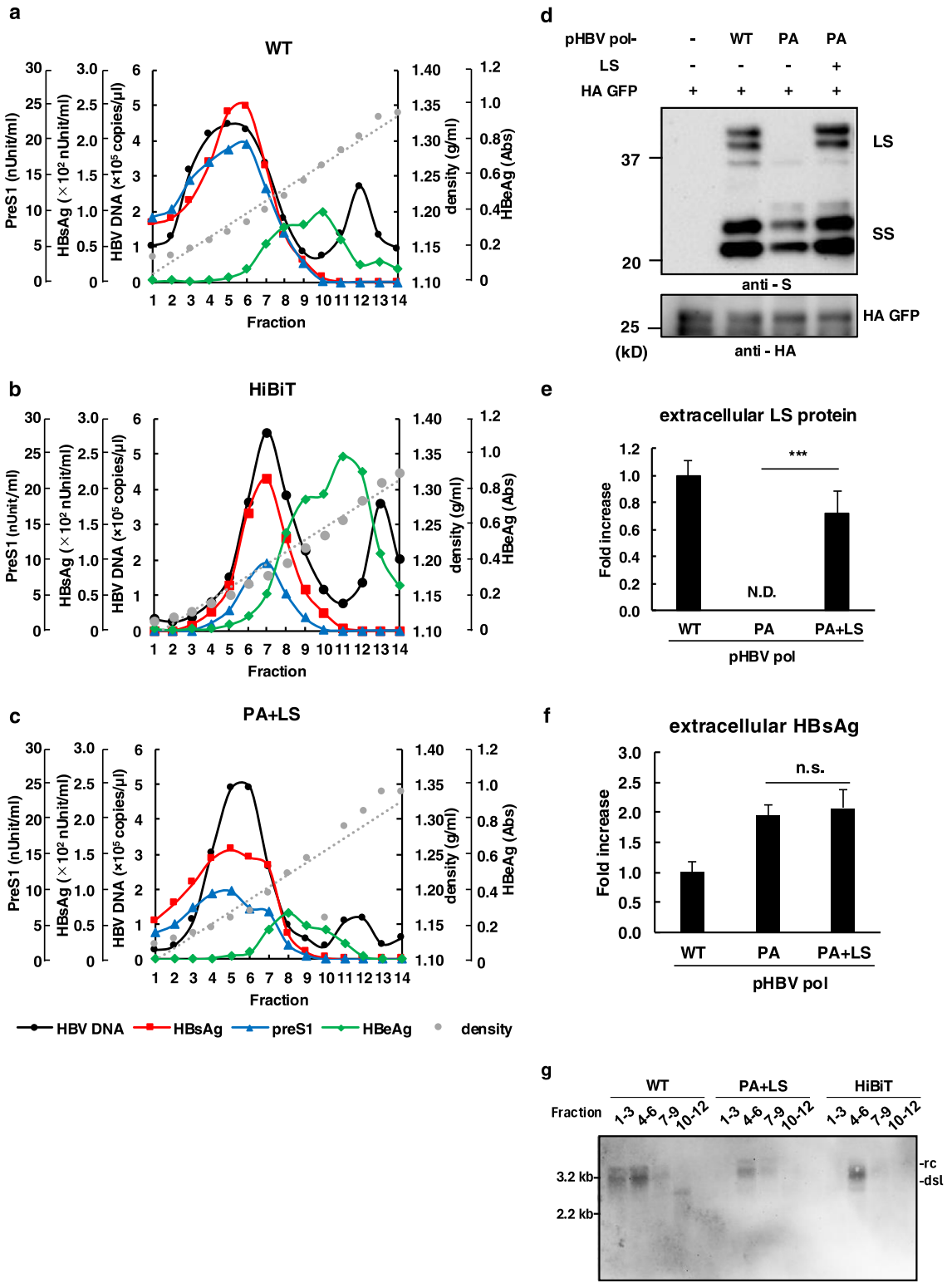

FIGURE 4 | Legend on next page.

rapid drug screening and tracking of viral dynamics [56–58]. Although recent advances in HBV reverse genetics have finally achieved the production of recombinant HBV (recHBV) particles carrying a variety of exogenous genes [25, 59–62], development of infectious and replication-competent recHBV seems to be very difficult due to size, structure, and gene organization of the HBV genome. Thus, insertion or replacement with foreign genes is extremely restricted. A previous report has shown that the recHBV encoding a reporter gene to monitor the early stage of the HBV replication cycle was successfully generated by trans-complementary expression of HBV pol [60], though the recHBV particles were replication-incompetent in infected cells. Looking at HBV genome and genes, there could be several sites where we could insert foreign genes if they were very small/short. These sites might be the C-terminal region of X ORF and preC region, though functional elements around here must be retained, such as direct repeat 1 and 2 (DR1, DR2) and enhancer II, a packaging signal ε [63]. The preS1 region overlapping with spacer region of HBVpol could be another candidate to insert short tags, though polymerase and preS1 amino acid frame must be considered carefully and insertion into preS1 region might affect infectivity [25, 64]. And some reports showed recHBV encoding a reporter tag in the preS1 region or preS2, allowing HBV to infect and replicate, has been more easily monitored [25, 59].

HBVpol, only a product with enzymatic activity among HBV genes, is responsible for a key process of reverse transcription in the HBV replication cycle. Its intracellular dynamics, however, has not been elucidated yet and it is important to understand the details for novel therapeutics development against HBV. HBVpol itself is very hard to study because overexpression and purification of HBVpol are difficult. Considering the fact, there is little structural information and HBVpol has not been detected and tracked yet.

In this study, we established replication-competent recHBV by focusing on the spacer domain of HBVpol for the following three reasons: (1) the spacer domain is unlikely to be functional as a reverse transcriptase; (2) it is low homology among HBV genotypes (a variable region); (3) LS protein (preS1), which overlaps the spacer domain of polymerase has two isoforms, one with 119 aa and another with 108 aa [8, 13, 15–17] and the first 11 amino acids seen in the 119 aa version of preS1 seems not to be essential. Actually, it was reported that a GTC strain with preS1 N-terminal deletion was isolated from HBV-infected patients, and such HBV GTC expressed 108 aa preS1 [40, 41], which resembles HBV GTD [65], whose preS1 is originally 108aa (GenBank # V01460.1). As mentioned, the N-terminal of preS1 seemed to be a potential region where short tags could be inserted. We constructed pol-PA and pol-HiBiT by replacing part of the spacer domain overlapping N-terminal of preS1 with PA- and HiBiT-tag, respectively (Figures 1a,2a), and investigated whether recHBV harboring pol-PA or pol-HiBiT were generated as infectious and replication-competent recHBV.

As a result, our constructed recHBV: HBV pol-PA and HBV pol-HiBiT were produced as infectious and replication-competent recHBV. These tagged HBVpol were detected visually and measured quantitively in the HBV replicating cells. IFA suggested co-localization between pol-PA and capsid (Figure 3a, b). However, it is unclear whether this pol-PA is encapsidated or not. Probably, nonionic detergent treatment to prepare capsids allows small molecules such as nucleotide [44, 66] but maybe not large molecules like antibodies. Thus, our data should show the co-localization of pol-PA and capsids during assembly. Otherwise, the higher resolution microscopy will resolve the problem.

HiBiT assay showed that the amount of intracellular pol-HiBiT was measurable in the transfection experiment (Figure 3c), and this suggested that pol-HiBiT could be an application for screening of anti-HBV drugs. On the other hand, it was impossible to show HiBiT activity in the infection experiment (Figure 5). This is probably because viruses obtained from the transient transfection experiment was not enough and the infection dose was too low to detect. A good production system such as HepAD 38.7 cells [67] with which viruses will be obtained abundantly should be established.

Unfortunately, in case of HBV pol-PA, 2.4 kb mRNA for LS was less expressed (Figure 2f). The reason was unclear, since the TATA box was presumed to be at about 60 bp and the transcription start site for 2.4 kb RNA to be at 42 bp upstream of preS1 ATG (Supporting Information S1: Figure S5) [68, 69], though the transcription activity could be damaged by the replacement. Although the level of extracellular LS proteins from pHBV pol-HiBiT

FIGURE 4 | Characterization of HBV particles harboring PA-pol or HiBiT-pol. (a–c) CsCl density gradient centrifugation of each HBV particles produced in the supernatant of cells transfected with pHBV vectors. (a) pHBV WT (WT), (b) pHBV pol-HiBiT (HiBiT) and (c) pHBV pol-PA + pLVSIN LS (PA + LS) were transfected into NTCP/G2 cells and 6 days after transfection, HBV particles in supernatants were collected and concentrated. After ultra centrifugation, samples were fractioned into fourteen fractions and the CsCl density (gray), the amount of HBV DNA (black), HBsAg (red), preS1 (blue) and HBeAg (green) were measured in each fraction. (d) Western blot of all S proteins expressed in the cells transfected with each pHBV vector. 48 h after co-transfection of each pHBV vector with either an LS expressing plasmid, pLVSIN LS (LS), or pLVSIN, an empty vector, cell lysates were prepared for SDS-PAGE followed by Western blot where an anti-S antibody was used for detection. HA GFP expression was used for normalization of transfection. (e) Relative LS expression in the supernatant of cells transfected with each pHBV vector. 6 days after co-transfection of each pHBV vector with either pLVSIN LS or pLVSIN, extracellular LS proteins were measured by preS1 ELISA. The amount of LS proteins was normalized by luciferase activity and shown as a relative expression level. Data were presented as a mean + SD. Asterisks indicate significant differences between cells (***$p < 0.001$). Non-detected result was described as "N.D.". (Tukey-Kramer test, $N = 3$). (f) Relative HBsAg expression in the supernatant of cells transfected with each HBV vector either with pLVSIN LS or pLVSIN. Extracellular HBsAg was measured by HBs ELISA. Expression of HBsAg was normalized by luciferase activity and shown as a relative expression. Data were presented as a mean + SD. Asterisks indicate significant differences between cells (**$p < 0.01$; ***$p < 0.001$). Nonsignificant difference was described as "n.s." (Tukey-Kramer test, $N = 3$). (g) Southern Blot of HBV DNA of the fractions in the CsCl density gradient. Fr.1-12 were divided into 4 fractions, Fr.1-3, Fr.4-6, Fr.7-9, and Fr.10-12. HBV DNA was extracted from the fractions as shown in the panel.

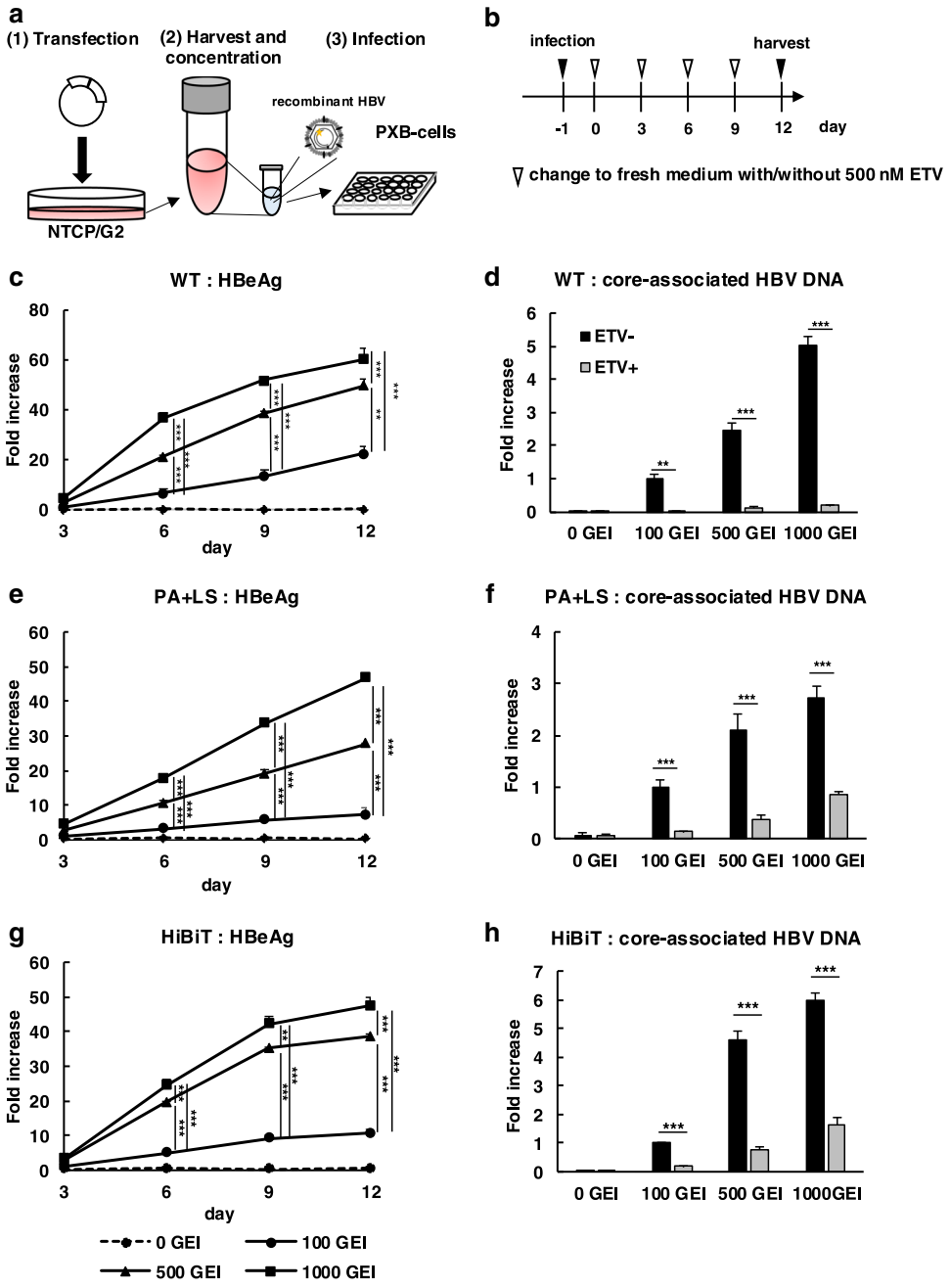

FIGURE 5 | Infection of HBV particles harboring pol-PA or pol-HiBiT to primary human hepatocytes. (a) Outline of the primary human hepatocytes (PXB cell) infection experiment. 6 days after transfection of each pHBV vector, the supernatants were harvested and concentrated. The titer of HBV particles was determined by qPCR, and then the virus solutions were used for HBV infection on PXB cell. (b) Time course of the PXB infection experiment. From a day after infection, culture medium was changed to fresh medium with or without 500 nM ETV every three days. 12 days after infection, samples were collected for analysis. HBV was infected with PXB cells at several GEI (0, 100, 500, and 1000) ($N = 3$ for each). (c, e, g) extracellular HBeAg secreted from the cells transfected with (c) pHBV pol-WT (WT), (e) pHBV pol-PA and LVSIN LS (PA + LS) and (g) pHBV pol-HiBiT (HiBiT) was monitored every 3 days for 12 days by ELISA. (d, f, h) core-associated HBV DNA in the lysate was measured at the end of infection, (d) pHBV pol-WT, (f) pHBV pol-PA and LVSIN LS and (h) pHBV pol-HiBiT. Data were presented as a mean + SD. Asterisks indicate significant differences between cells (*$p < 0.05$; **$p < 0.01$; ***$p < 0.001$). Nonsignificant difference was described as "n.s." (Dunnet test).

transfected NTCP/G2 cells seemed to be reduced (Figure 2e), mature HBV pol-HiBiT was successfully produced (Figure 4b,g). There is a possibility that the insertion could affect 2.4 kb mRNA transcription machinery. Furthermore, we constantly observed less expression of intracellular SS in pHBV pol-PA transfection experiment (Figure 4d, the upper panel). Since extracellular expression of HBsAg was comparable among three constructs; pHBV pol-WT, pol-PA, and pol-HiBiT 48 h after-transfection (Figure 2d), we speculate that the lower expression of LS protein from pHBV pol-PA might facilitate HBsAg secretion. Although there could be better alternatives for insertion/replication sites in the preS1 region and for the tags itself, HBV pol-PA was successfully produced from pHBV pol-PA by trans-complementation of LS protein (Figures 4c–e and Supporting Information S1: S4).

In conclusion, our studies demonstrated that insertion of short tags into the spacer domain of HBVpol allowed production of infectious and replication-competent recHBV, which could be visualized and quantified in the replicating cells. This study opens up new avenues for the precise research of HBVpol and development of new therapeutics against HBV.

Author Contributions

C.M. and K.U. designed the experiments. C.M. performed the experiments. C.M., M.W., E.O., S.K. and K.U. discussed the data; and C.M., M.W., E.O., S.K., and K.U. wrote the manuscript. K.U. also supervised this study.

Acknowledgments

This research was supported by Grants from the Japan Agency for Medical Research and Development (AMED) Grants (16fk031050 4h0005, 17fk0310105h0001, 18fk0310105h0002, 19fk0310105h0003, 20fk 0310105h0004, 21fk0310105h005, 22fk0310505h0001, 23fk0310505h0002, and 24fk0310505h003) to K.U. and from JST SPRING, Grant Number JPMJSP2138, to C.M. and from the Osaka University Transdisciplinary Program for Biomedical Entrepreneurship and Innovation (WISE program) to C.M. We would like to thank Ms. H. Ohtake, Ms. H. Kawakami and Ms. N. Hashimoto for their technical support and Dr. C. Ono and Dr. Y. Matsuura from RIMD and CiDER for providing plasmid. We also would like to thank Dr. K. Miyakawa and Dr. A. Ryo from NIID for providing the anti-pol antibody. Finally, we would like to thank Leica Imaging Center at FBS Core Facility in Osaka University for technical support.

Conflicts of Interest

The authors declare that the research was conducted in the absence of any commercial or financial relationship that could be construed as a potential conflict of interest.

Disclosure

None.

Data Availability Statement

The data sets generated for this study are available on request to the corresponding author.

References

1. WHO. Global Progress Report on HIV, Viral Hepatitis and Sexually Transmitted Infections. 2021.

2. W. J. Jeng, G. V. Papatheodoridis, and A. S. F. Lok, "Hepatitis B," *The Lancet* 401, no. 10381 (2023): 1039–1052.

3. A. Schweitzer, J. Horn, R. T. Mikolajczyk, G. Krause, and J. J. Ott, "Estimations of Worldwide Prevalence of Chronic Hepatitis B Virus Infection: A Systematic Review of Data Published Between 1965 and 2013," *The Lancet* 386, no. 10003 (2015): 1546–1555.

4. J. L. Dienstag, "Hepatitis B Virus Infection," *New England Journal of Medicine* 359, no. 14 (2008): 1486–1500.

5. C. Seeger and W. S. Mason, "Molecular Biology of Hepatitis B Virus Infection," *Virology* 479–480 (2015): 672–686.

6. G. H. Wang, F. Zoulim, E. H. Leber, J. Kitson, and C. Seeger, "Role of RNA in Enzymatic Activity of the Reverse Transcriptase of Hepatitis B Viruses," *Journal of Virology* 68, no. 12 (1994): 8437–8442.

7. L. Stuyver, "Nomenclature for Antiviral-Resistant Human Hepatitis B Virus Mutations in the Polymerase Region," *Hepatology* 33, no. 3 (2001): 751–757.

8. G. Radziwill, W. Tucker, and H. Schaller, "Mutational Analysis of the Hepatitis B Virus P Gene Product: Domain Structure and RNase H Activity," *Journal of Virology* 64, no. 2 (1990): 613–620.

9. H. Toh, H. Hayashida, and T. Miyata, "Sequence Homology Between Retroviral Reverse Transcriptase and Putative Polymerases of Hepatitis B Virus and Cauliflower Mosaic Virus," *Nature* 305, no. 5937 (1983): 827–829.

10. R. E. Lanford, L. Notvall, H. Lee, and B. Beames, "Transcomplementation of Nucleotide Priming and Reverse Transcription Between Independently Expressed TP and RT Domains of the Hepatitis B Virus Reverse Transcriptase," *Journal of Virology* 71, no. 4 (1997): 2996–3004.

11. F. Zoulim and C. Seeger, "Reverse Transcription in Hepatitis B Viruses is Primed by a Tyrosine Residue of the Polymerase," *Journal of Virology* 68, no. 1 (1994): 6–13.

12. M. Weber, V. Bronsema, H. Bartos, A. Bosserhoff, R. Bartenschlager, and H. Schaller, "Hepadnavirus P Protein Utilizes a Tyrosine Residue in the TP Domain to Prime Reverse Transcription," *Journal of Virology* 68, no. 5 (1994): 2994–2999.

13. C. Pley, J. Lourenço, A. L. McNaughton, and P. C. Matthews, "Spacer Domain in Hepatitis B Virus Polymerase: Plugging a Hole or Performing a Role?," *Journal of Virology* 96, no. 9 (2022): e0005122.

14. L. Wei and A. Ploss, "Core Components of DNA Lagging Strand Synthesis Machinery Are Essential for Hepatitis B Virus cccDNA Formation," *Nature Microbiology* 5, no. 5 (2020): 715–726.

15. P. Chen, Y. Gan, N. Han, et al., "Computational Evolutionary Analysis of the Overlapped Surface (S) and Polymerase (P) Region in Hepatitis B Virus Indicates the Spacer Domain in P is Crucial for Survival," *PLoS One* 8, no. 4 (2013): e60098.

16. Y. Kim, Y. B. Hong, and G. Jung, "Hepatitis B Virus: DNA Polymerase Activity of Deletion Mutants," *IUBMB Life* 47, no. 2 (1999): 301–308.

17. Li. J. S. Fourel, I. Jaquet, and C. Trépo, "C. Decreased Replication Capacity of a Duck Hepatitis B Virus Mutant With Altered Distal Pre-S Region," *Virus Res* 20, no. 1 (1991): 11–21.

18. S. A. Jones, R. Boregowda, T. E. Spratt, and J. Hu, "In Vitro Epsilon RNA-Dependent Protein Priming Activity of Human Hepatitis B Virus Polymerase," *Journal of Virology* 86, no. 9 (2012): 5134–5150.

19. L. J. Chang, R. C. Hirsch, D. Ganem, and H. E. Varmus, "Effects of Insertional and Point Mutations on the Functions of the Duck Hepatitis B Virus Polymerase," *Journal of Virology* 64, no. 11 (1990): 5553–5558.

20. X. Wei and D. L. Peterson, "Expression, Purification, and Characterization of an Active RNase H Domain of the Hepatitis B Viral Polymerase," *Journal of Biological Chemistry* 271, no. 51 (1996): 32617–32622.

21. J. Summers and W. S. Mason, "Replication of the Genome of a Hepatitis B-Like Virus by Reverse Transcription of an RNA Intermediate," *Cell* 29, no. 2 (1982): 403–415.

22. D. N. Clark and J. Hu, "Unveiling the Roles of HBV Polymerase for New Antiviral Strategies," *Future Virology* 10, no. 3 (2015): 283–295.

23. J. Hu and C. Seeger, "Hepadnavirus Genome Replication and Persistence," *Cold Spring Harbor Perspectives in Medicine* 5, no. 7 (2015): a021386.

24. A. Murayama, H. Igarashi, N. Yamada, et al., "Exploring the Tolerable Region for HiBiT Tag Insertion in the Hepatitis B Virus Genome," *mSphere* 9 (2024): e0051824.

25. A. Sumiyadorj, K. Murai, T. Shimakami, et al., "A Single Hepatitis B Virus Genome With a Reporter Allows the Entire Viral Life Cycle to be

Monitored in Primary Human Hepatocytes," *Hepatology Communications* 6, no. 9 (2022): 2441–2454.

26. M. Yoshita, M. Funaki, T. Shimakami, et al., "High-Throughput Screening of Antiviral Compounds Using a Recombinant Hepatitis B Virus and Identification of a Possible Infection Inhibitor, Skimmianine," *Viruses* 16, no. 8 (2024): 1346.

27. T. Mu, X. Zhao, Y. Zhu, H. Fan, and H. Tang, "The E3 Ubiquitin Ligase TRIM21 Promotes HBV DNA Polymerase Degradation," *Viruses* 12, no. 3 (2020): 346.

28. Y. Yao, B. Yang, Y. Chen, et al., "RNA-Binding Motif Protein 24 (RBM24) Is Involved in Pregenomic RNA Packaging by Mediating Interaction Between Hepatitis B Virus Polymerase and the Epsilon Element," *Journal of Virology* 93, no. 6 (2019): e02161-18, https://doi.org/10.1128/JVI.02161-18.

29. M. Iwamoto, K. Watashi, S. Tsukuda, et al., "Evaluation and Identification of Hepatitis B Virus Entry Inhibitors Using HepG2 Cells Overexpressing a Membrane Transporter NTCP," *Biochemical and Biophysical Research Communications* 443, no. 3 (2014): 808–813.

30. C. Yamasaki, M. Kataoka, Y. Kato, et al., "In Vitro Evaluation of Cytochrome P450 and Glucuronidation Activities in Hepatocytes Isolated From Liver-Humanized Mice," *Drug Metabolism and Pharmacokinetics* 25, no. 6 (2010): 539–550.

31. M. G. Hossain, Y. Suwanmanee, K. Du, and K. Ueda, "Analysis of the Physicochemical Properties, Replication and Pathophysiology of a Massively Glycosylated Hepatitis B Virus HBsAg Escape Mutant," *Viruses* 13, no. 11 (2021): 2328.

32. A. Fujiyama, A. Miyanohara, C. Nozaki, T. Yoneyama, N. Ohtomo, and K. Matsubara, "Cloning and Structural Analyses of Hepatitis B Virus DNAs, Subtype ADR," *Nucleic Acids Research* 11, no. 13 (1983): 4601–4610.

33. Y. Fauzyah, C. Ono, S. Torii, et al., "Ponesimod Suppresses Hepatitis B Virus Iinfection by Inhibiting Endosome Maturation," *Antiviral Research* 186 (2021): 104999.

34. M. Sugiyama, Y. Tanaka, T. Kato, et al., "Influence of Hepatitis B Virus Genotypes on the Intra- and Extracellular Expression of Viral DNA and Antigens," *Hepatology* 44, no. 4 (2006): 915–924.

35. E. M. M. Manders, F. J. Verbeek, and J. A. Aten, "Measurement of Co-Localization of Objects in Dual-Colour Confocal Images," *Journal of Microscopy* 169, no. 3 (1993): 375–382.

36. E. M. M. Manders, J. Stap, G. J. Brakenhoff, R. V. Driel, and J. A. Aten, "Dynamics of Three-Dimensional Replication Patterns During the S-phase, Analysed by Double Labelling of DNA and Confocal Microscopy," *Journal of Cell Science* 103, no. Pt 3 (1992): 857–862.

37. Y. Ishida, C. Yamasaki, A. Yanagi, et al., "Novel Robust in Vitro Hepatitis B Virus Infection Model Using Fresh Human Hepatocytes Isolated From Humanized Mice," *The American Journal of Pathology* 185, no. 5 (2015): 1275–1285.

38. Y. Fujii, M. Kaneko, M. Neyazaki, T. Nogi, Y. Kato, and J. Takagi, "PA Tag: A Versatile Protein Tagging System Using a Super High Affinity Antibody Against a Dodecapeptide Derived From Human Podoplanin," *Protein Expression and Purification* 95 (2014): 240–247.

39. Y. Kato, M. K. Kaneko, A. Kuno, et al., "Inhibition of Tumor Cell-Induced Platelet Aggregation Using a Novel Anti-Podoplanin Antibody Reacting With Its Platelet-aggregation-Stimulating Domain," *Biochemical and Biophysical Research Communications* 349, no. 4 (2006): 1301–1307.

40. W. H. Choe, H. Kim, S. Y. Lee, et al., "Three Types of PreS1 Start Codon Deletion Variants in the Natural Course of Chronic Hepatitis B Infection," *Journal of Gastroenterology and Hepatology* 33, no. 7 (2018): 1370–1378.

41. S. A. Lee, "Hepatitis B Virus preS1 Deletion is Related to Viral Replication Increase and Disease Progression," *World Journal of Gastroenterology* 21, no. 16 (2015): 5039–5048.

42. G. Ou, L. He, L. Wang, et al., "The Genotype (A to H) Dependent N-Terminal Sequence of HBV Large Surface Protein Affects Viral Replication, Secretion and Infectivity," *Frontiers in Microbiology* 12 (2021): 687785.

43. A. Murayama, N. Yamada, Y. Osaki, et al., "N-Terminal PreS1 Sequence Regulates Efficient Infection of Cell-Culture-Generated Hepatitis B Virus," *Hepatology* 73, no. 2 (2021): 520–532.

44. M. Junker-Niepmann, R. Bartenschlager, and H. Schaller, "A Short Cis-Acting Sequence is Required for Hepatitis B Virus Pregenome Encapsidation and Sufficient for Packaging of Foreign RNA," *The EMBO Journal* 9, no. 10 (1990): 3389–3396.

45. R. C. Hirsch, J. E. Lavine, L. Chang, H. E. Varmus, and D. Ganem, "Polymerase Gene Products of Hepatitis B Viruses Are Required for Genomic RNA Packaging as Well as for Reverse Transcription," *Nature* 344, no. 6266 (1990): 552–555.

46. R. Bartenschlager, M. Junker-Niepmann, and H. Schaller, "The P Gene Product of Hepatitis B Virus Is Required as a Structural Component for Genomic RNA Encapsidation," *Journal of Virology* 64, no. 11 (1990): 5324–5332.

47. J. F. Conway, N. R. Watts, D. M. Belnap, et al., "Characterization of a Conformational Epitope on Hepatitis B Virus Core Antigen and Quasiequivalent Variations in Antibody Binding," *Journal of Virology* 77, no. 11 (2003): 6466–6473.

48. J. S. Aaron, A. B. Taylor, and T. L. Chew, "Image Co-Localization-Co-Occurrence Versus Correlation," *Journal of Cell Science* 131, no. 3 (2018): jcs211847, https://doi.org/10.1242/jcs.211847.

49. R. Hong, W. Bai, J. Zhai, et al., "Novel Recombinant Hepatitis B Virus Vectors Efficiently Deliver Protein and RNA Encoding Genes Into Primary Hepatocytes," *Journal of Virology* 87, no. 12 (2013): 6615–6624.

50. C. Tateno, Y. Kawase, Y. Tobita, et al., "Generation of Novel Chimeric Mice With Humanized Livers by Using Hemizygous cDNA-uPA/SCID Mice," *PLoS One* 10, no. 11 (2015): e0142145.

51. C. Tateno, Y. Yoshizane, N. Saito, et al., "Near Completely Humanized Liver in Mice Shows Human-Type Metabolic Responses to Drugs," *The American Journal of Pathology* 165, no. 3 (2004): 901–912.

52. P. A. Revill, F. V. Chisari, J. M. Block, et al., "A Global Scientific Strategy to Cure Hepatitis B," *The Lancet Gastroenterology & Hepatology* 4, no. 7 (2019): 545–558.

53. T. Suzuki and A. Saito, "Advances in the Reverse Genetics System for RNA Viruses," *Folia Pharmacologica Japonica* 157, no. 2 (2022): 134–138.

54. V. R. Racaniello and D. Baltimore, "Cloned Poliovirus Complementary DNA is Infectious in Mammalian Cells," *Science* 214, no. 4523 (1981): 916–919.

55. A. Adachi, H. E. Gendelman, S. Koenig, et al., "Production of Acquired Immunodeficiency Syndrome-Associated Retrovirus in Human and Nonhuman Cells Transfected With an Infectious Molecular Clone," *Journal of Virology* 59, no. 2 (1986): 284–291.

56. X. Xie, A. E. Muruato, X. Zhang, et al., "A Nanoluciferase SARS-CoV-2 for Rapid Neutralization Testing and Screening of Anti-Infective Drugs for COVID-19," *Nature Communications* 11, no. 1 (2020): 5214.

57. T. Tamura, T. Fukuhara, T. Uchida, et al., "Characterization of Recombinant Flaviviridae Viruses Possessing a Small Reporter Tag," *Journal of Virology* 92, no. 2 (2018): e01582-17, https://doi.org/10.1128/JVI.01582-17.

58. J. W. Schoggins, M. Dorner, M. Feulner, et al., "Dengue Reporter Viruses Reveal Viral Dynamics in Interferon Receptor-Deficient Mice and Sensitivity to Interferon Effectors in Vitro," *Proceedings of the National Academy of Sciences* 109, no. 36 (2012): 14610–14615.

59. Y. Nakaya, D. Onomura, Y. Hoshi, et al., "Establishment of a Hepatitis B Virus Reporter System Harboring a HiBiT-tag in the PreS2 Region," *Journal of Infectious Diseases* (2024): jiae353, https://doi.org/10.1093/infdis/jiae353.

60. H. Nishitsuji, S. Ujino, Y. Shimizu, et al., "Novel Reporter System to Monitor Early Stages of the Hepatitis B Virus Life Cycle," *Cancer Science* 106, no. 11 (2015): 1616–1624.

61. Z. Wang, L. Wu, X. Cheng, et al., "Replication-Competent Infectious Hepatitis B Virus Vectors Carrying Substantially Sized Transgenes by Redesigned Viral Polymerase Translation," *PLoS One* 8, no. 4 (2013): e60306.

62. S. Chaisomchit, D. Tyrrell, and L. J. Chang, "Development of Replicative and Nonreplicative Hepatitis B Virus Vectors," *Gene Therapy* 4, no. 12 (1997): 1330–1340.

63. J. Wang, H. Huang, Y. Liu, et al., "HBV Genome and Life Cycle," *Advances in Experimental Medicine and Biology* 1179 (2020): 17–37.

64. H. Yan, G. Zhong, G. Xu, et al., "Sodium Taurocholate Cotransporting Polypeptide is a Functional Receptor for Human Hepatitis B and D Virus," *Elife* 1 (2012): e00049.

65. F. Galibert, E. Mandart, F. Fitoussi, P. Tiollais, and P. Charnay, "Nucleotide Sequence of the Hepatitis B Virus Genome (Subtype AYW) Cloned in E. coli," *Nature* 281, no. 5733 (1979): 646–650.

66. W. S. Mason, G. Seal, and J. Summers, "Virus of Pekin Ducks With Structural and Biological Relatedness to Human Hepatitis B Virus," *Journal of Virology* 36, no. 3 (1980): 829–836.

67. S. K. Ladner, M. J. Otto, C. S. Barker, et al., "Inducible Expression of Human Hepatitis B Virus (HBV) in Stably Transfected Hepatoblastoma Cells: A Novel System for Screening Potential Inhibitors of HBV Replication," *Antimicrobial Agents and Chemotherapy* 41, no. 8 (1997): 1715–1720.

68. N. Moolla, M. Kew, and P. Arbuthnot, "Regulatory Elements of Hepatitis B Virus Transcription," *Journal of Viral Hepatitis* 9, no. 5 (2002): 323–331.

69. A. Siddiqui, S. Jameel, and J. Mapoles, "Transcriptional Control Elements of Hepatitis B Surface Antigen Gene," *Proceedings of the National Academy of Sciences* 83, no. 3 (1986): 566–570.

Supporting Information

Additional supporting information can be found online in the Supporting Information section.